Desalination and Water Treatment
www.deswater.com
doi: 10.1080/19443994.2013.797367

52 (2014) 2372–2381
March

Taylor & Francis
Taylor & Francis Group

Production of drinking water from seawater using membrane distillation (MD) alternative: direct contact MD and sweeping gas MD approaches

Mohammad Mahdi A. Shirazi[a], Ali Kargari[b,*], Dariush Bastani[c], Leila Fatehi[d]

[a]*Young Researchers and Elites Club, Omidieh Branch, Islamic Azad University, Omidieh, P.O. Box 164, Iran*
[b]*Membrane Processes Research Laboratory (MPRL), Petrochemical Engineering Department, Amirkabir University of Technology (Tehran Polytechnic), Mahshahr Campus, Mahshahr, Iran*
Tel./Fax: +98 6522342779; email: kargari@aut.ac.ir
[c]*Department of Chemical and Petroleum Engineering, Sharif University of Technology, Tehran, Iran*
[d]*Department of Chemical Engineering, Science and Research Branch, Islamic Azad University, Tehran, Iran*

Received 16 November 2012; Accepted 7 April 2013

ABSTRACT

In this work, two-membrane distillation (MD) modes, direct contact MD, and sweeping gas MD were investigated for synthesized and real (Persian Gulf) seawater desalination. A commercial PTFE membrane with 0.22 μm pore size was characterized (using atomic force microscopy and scanning electron microscopy) and was used for experiments. A multipurpose plate and frame MD module was used for desalination experiments. The effects of various operating conditions and MD module design, as well as feed type on the permeation flux have been studied. The feed temperature was found to be the most effective operating parameter. The flow rate in both sides of the MD module was found to be effective; however, the feed flow rate showed more influence. Both the investigated modes were successfully applied for seawater desalination, whilst the direct contact mode seems to provide more permeation flux. The results indicated that the MD module design has significant effect on the overall efficiency. At optimum conditions, a 99% salt rejection was achieved for both the investigated MD modes.

Keywords: Desalination; Drinking water; Persian Gulf seawater; Direct contact MD; Sweeping gas MD; PTFE membrane; Module design; Permeation flux

1. Introduction

Today world's demand for freshwater cannot be met further by the available conventional energy sources, such as oil and gas. Therefore, technologies which use renewable energy and/or waste heat sources for water desalination will fill an important niche. In dry regions like those of the Persian Gulf and Sistan Sea regions (in the south of Iran and the north of Arabian countries), the situation is the worst since the freshwater demand is mostly met by thermal-based desalination plants and/or pressure-driven membrane processes, all the mentioned desalination processes are driven by fossil fuels.

*Corresponding author.

1944-3994/1944-3986 © 2013 Balaban Desalination Publications. All rights reserved.

The continued research for efficient, cost-effective, and energy-saving technology to produce freshwater from saline and polluted resources has introduced a new hybrid process, a combination of traditional distillation and membrane separation, which is called "Membrane distillation". Membrane distillation (MD) is a versatile nonisothermal membrane process for separations that are mainly suited for applications in which water is the major component present in the feed stream to be treated, such as desalination [1,2]. MD refers to a thermal-driven transport of vapor through a microporous hydrophobic membrane. The MD's driving force is the partial pressure difference between each side of the membrane's pores [3–5].

MD is considered as one of the technologies that is versatile and an attractive alternative desalination process. Various researchers have reviewed the details of the MD process [4–11]. It holds the potential of being a cost-effective, eco-efficient, and emerging desalination technique that can utilize renewable and low-grade energy resources, such as solar or geothermal energies, which are widely available in the Persian Gulf region and Middle East [12–16].

A variety of the methods have been used to impose the driving force and improve the permeation flux that include direct contact MD (DCMD) (which is the most investigated MD mode), air-gap MD, vacuum MD, and sweeping gas membrane distillation (SGMD) (which in contrast with DCMD is the least considered MD's configuration) [9]. The main difference in these configurations consists of the type of the condensing (permeate side) design [8,11].

Among other applications of MD process [8,10,17], most of the researches have been focused on desalination and treatment of water and wastewater resources [4,11]. Most of these researches have used the commercially available hydrophobic microporous membranes, which specifically are fabricated for microfiltration purposes [9]. The important characteristics of these commercial membranes which are required for a suitable MD membrane, such as excellent mechanical and chemical resistance, thermal stability, high liquid entry pressure, high porosity, high hydrophobicity, low thermal conductivity, and narrow pore size distribution have been reported extensively [17–23]. However, there are still some issues that have not yet been clearly answered, such as, are the current reported MD flux limited by the membrane or by the process parameters and module design? A detailed discussion on these issues is highlighted in this paper.

The main potential challenges towards the MD process, especially for desalination purpose; reduce the conductive losses in order to maintain the flux stability over time, avoid pore-wetting, and minimize the concentration and temperature polarizations that have been reported in detail [1,2,4,5,9,11]. Most of the references identified in these studies used commercial hydrophobic membrane as well as distilled water and/or synthetic saline solutions (NaCl solution) as feed in their experiments. In the authors' opinion, such feed might not provide an accurate indication of the capability of the commercial membranes to desalinate real seawater. However, there are few reported works using real seawater as feed for MD experiments, but the obtained flux performances were low compared with synthetic seawater [18].

In this work, the aim is partially to answer the question on the expected satisfactory flux in MD by subjecting two configurations (DCMD and SGMD) and a commercial PTFE membrane for the desalination of Persian Gulf seawater. A number of experiments on seawater desalination were conducted through DCMD and SGMD configurations using a multipurpose experimental MD set-up. The effects of operating conditions, MD module design, and feed type as well as flux variation for each MD mode were studied and the obtained results were compared.

2. Materials and methods

2.1. Materials

The feed samples were synthesized seawater (NaCl solution) and real seawater from Persian Gulf seaside (provided from South Pars Energy Zone in the south of Iran). Table 1 shows the composition of the applied

Table 1
Persian Gulf seawater analysis (South Pars Energy Zone seaside in the south of Iran)

Item	Value	Unit
pH	7.5	–
Calcium as Ca	493	ppm
Magnesium as Mg	1,231	ppm
Sodium as Na	10,334	ppm
Potassium as K	388	ppm
Ammonia as NH_4	0.01	ppm
Chloride as Cl	19,622	ppm
Sulfate as SO_4	1998	ppm
Silica as SiO_2	0.14	ppm
Solid total Fe	0.025	ppm
Solid total Mn	0.09	ppm
Suspended solids	12.8	ppm
Total salt content	35,878	ppm
Conductivity at 20°C	47,410	μS/cm

Table 2
Characteristics of the membrane used for the present study

Pore size (μm)	Water flow rate $\left(\frac{mL}{min\,cm^2}\right)$	Bubble point (psi)	Thickness (μm)	Porosity (%)
0.22[a]	15[a]	14.8–20.9[a,b]	175[a]	70[a]

[a]Reported by manufacturer.
[b]@ 23 °C for air with methanol.

real seawater. A hydrophobic membrane made of PTFE (Millipore, USA) with 0.22 μm pore size was used for the experiments. Table 2 shows the characteristics of the applied membrane.

2.2. Experimental set-up

A multipurpose MD set-up was designed and used for the experiments. The apparatus equipped by a plate and a frame membrane module with 0.0169 m^2 ($130 \times 130 \times 3$ mm) effective area for DCMD and SGMD experiments; two diaphragm pumps (So∼Pure, Korea), one for re-circulation of the hot feed in the closed loop of feed tank-MD module-feed tank for both modes, and another for re-circulation of the condensing fluid in DCMD mode (Fig. 1(a)); two precision flow-meters (Brooks, Netherlands); an oil-free compressor (GAST, USA), and a cold trap equipped with a refrigerator system to provide the sweeping gas (SG) and condensing the permeate stream in SGMD mode (Fig. 1(b)), respectively, an PID controller for temperature adjustment; five thermal sensors (Pt-100) for temperature monitoring at four inlet and outlet points, and feed tank; a double-layer stainless steel feed tank equipped by an over-head mixer in order to homogenize the concentration and temperature in the feed tank.

2.3. Experimental procedure

Data were logged every 30 min during 180-min run duration, the experiments were repeated three times, and then the average results were reported. The membrane was first soaked in absolute ethanol for 1 h, then washed and soaked in distilled water for at least for 2 h and again soaked in absolute ethanol for 1 h again, and the membrane was used after drying its both sides at least for 10 min using a hot dried air stream (60 °C). This is a standard procedure for cleaning the pores of virgin hydrophobic membranes prior to MD tests. This pretreatment procedure for the

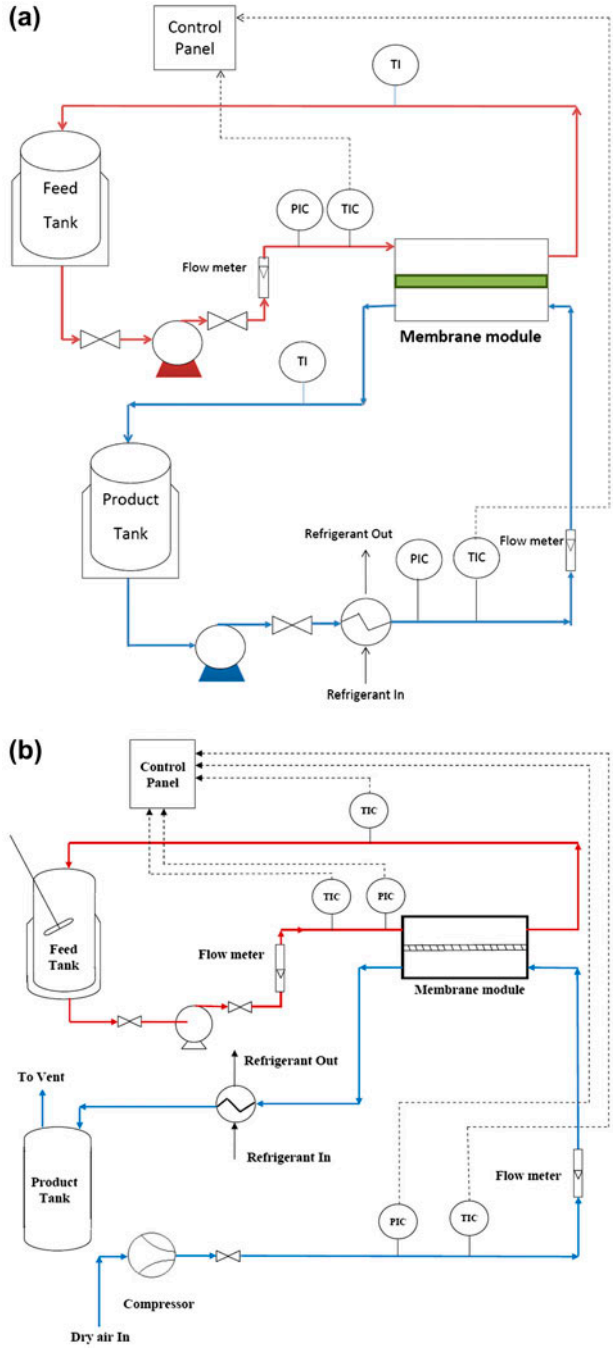

Fig. 1. A general scheme of the DCMD (a) and SGMD (b) apparatus applied in this work.

applied membrane was selected because during our preliminary investigations, we realized that by using this precleaning procedure, the commercial membranes have better performance. Therefore, the readers are recommended to use this procedure prior to applying the commercial hydrophobic PTFE membranes for MD purposes. In all the tests conducted, the active layer of membrane faced the hot feed.

The performance of membrane separation processes is usually evaluated by the permeation flux which is defined as the mass or volume (kg or L) of permeate collected per the membrane active area (m^2) and operation time (h). In this work, the permeation flux is considered as the target parameter on which the effects of operating variables should be evaluated.

2.4. Analysis

The feed and permeate compositions were measured using an EC470-L EC-meter (ISTEK, Korea). Scanning electron microscopy (SEM) (VEGA, TESCAN, Czech Republic) and atomic force microscopy (AFM) (DUALSCOP 95-200E, DEM, Denmark) were used for the morphological observation of the virgin membrane. Hydrophobicity was tested by a contact angle measuring system (KRUSS G-10, Germany).

3. Results and discussion

3.1. Membrane characterization

As mentioned earlier, most of the applied membranes in MD process are those that are made up of hydrophobic polymers and are specifically fabricated for microfiltration purposes [9]. Therefore, characterization of these commercial hydrophobic membranes prior to any MD test is necessary for in-depth understanding and predicting their performance. Fig. 2 shows the SEM and AFM images of the applied membrane. One of the parameters should be considered in morphological study of membranes is the pore-size distribution. In order to measure this parameter, inspecting line profiles analyzing on the AFM images at different locations of the membrane surface was considered. Fig. 3 shows the pore-size distribution (percentage of the pore-size values) for the applied PTFE membrane. As could be observed, about 50% of pore sizes are in the range of 0.2–0.3 μm, which is really close to the reported value (0.22 μm). Some pores of higher range are observed and about 15% of pores were below the 0.2 μm. It could be concluded by the following discussion. The PTFE membrane has very low solubility in chemical solvents; therefore, it usually fabricates via film-stretching method and as it could be observed in SEM image, the membrane has noncircular pore structure. Although, the larger pore could reduce the membrane performance, very low surface energy of PTFE polymer that leads to higher hydrophobicity reduces this weak point. The hydrophobicity of the membrane was measured based on the static water-drop contact angle for three times and an average value of $132.5^\circ \pm 0.1^\circ$ was estimated.

Surface roughness is another important membrane property which could directly affect the surface hydrophobicity [24,25]. Therefore, various roughness parameters, such as the mean roughness (R_a), the root mean square of Z data (R_q), and the mean difference in the height between the five highest peaks and the five lowest valleys (R_z) were measured. The parameters were obtained from the AFM images of different locations taken from the membrane sample (2×2 cm), and the average values were reported. R_a represents the mean value of the surface relative to the center plane for which the volumes enclosed by the images above and below this plane are equal. R_q is the standard deviation of the Z values within the specific

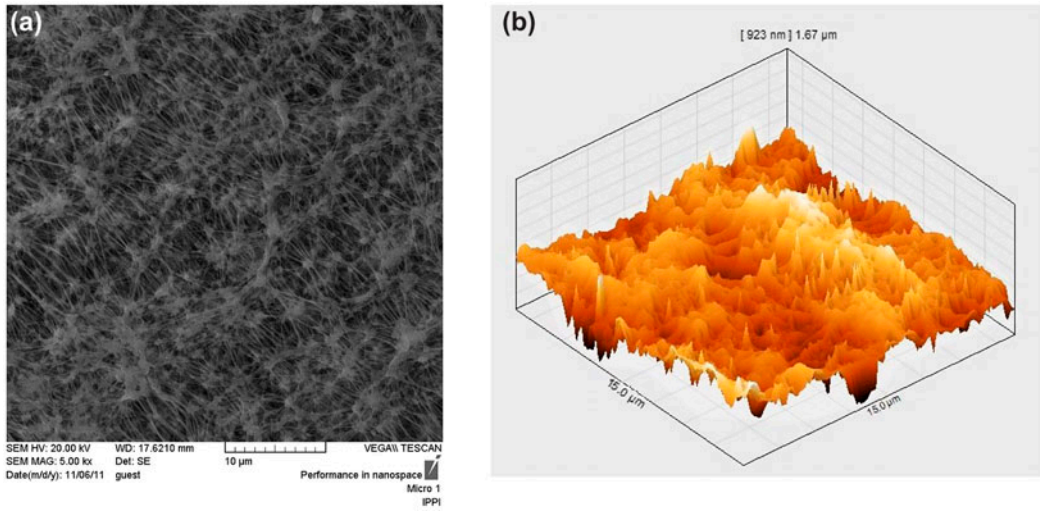

Fig. 2. SEM (a) and AFM (b) images of applied membrane.

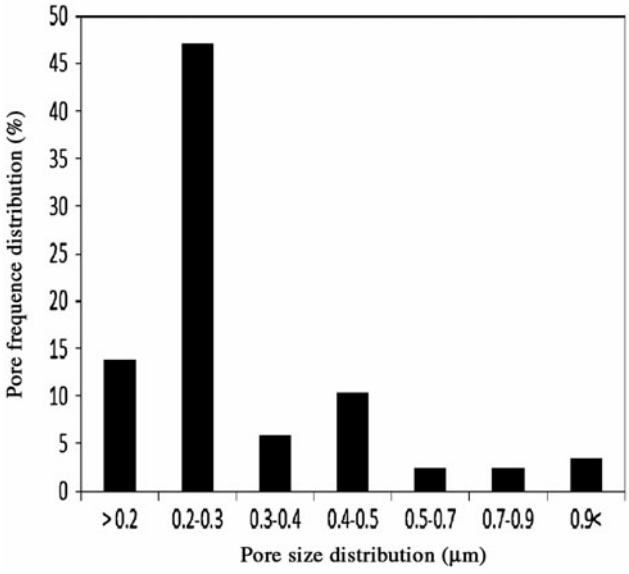

Fig. 3. Pore-size distribution of the applied membrane.

Table 3
Contact angle and roughness parameters measured for the applied membrane

Chemistry	Water contact angle (°)	R_a (nm)	R_q (nm)	R_z (nm)
Hydrophobic PTFE	132.5 ± 0.1	128 ± 0.5	154 ± 0.7	681 ± 0.4

area. Table 3 shows these roughness parameters. Further information on the detailed description of roughness parameters could be found in the previous work [21].

As could be observed in three-dimensional AFM image (Fig. 2), the membrane surface is not smooth and some nodule aggregates are observed. The nodules are seen as bright high peaks, while pores are seen as darker depressions. As mentioned earlier, PTFE membranes usually fabricate via film-stretching method; therefore, pores are not necessarily circular. Thus, the average of their length and width is usually recorded as pore size. The results obtained in this section could help to better understand the commercial PTFE membrane performance when it used for MD desalination purpose.

3.2. Effect of operating parameters

Obviously, feed temperature on the hot side of the MD module (T_h) should be investigated as the first operating variable due to the nature of MD process, which is a thermally-driven separation technique [4]. Fig. 4 shows the effect of the feed temperatures (40, 60, and 80°C) on the permeation flux for two configurations, DCMD and SGMD. As could be observed; the higher the feed temperature, the higher the permeation flux achieved. This can be explained by the exponential dependency of the vapor pressure from temperature based on the well-known Antoine's equation (feed temperature in MD) [5]. Consequently, higher mass transfer rate is expected when higher level of feed temperature is used. As could be observed, increasing the feed temperature had same effect on increase the permeation flux for both configurations, but with different responses. Increasing the feed temperature from 60 to 80°C was more effective than increasing it from 40 to 60°C. However, choosing the most-influence feed temperature depends on the available energy source, which can be solar, wind, or even waste heat energy in industrial units [11]. Based on the obtained results, feet temperature of 80°C was adopted for next experiments.

Feed flow rate (200, 400, 600, and 800 mL/min) was investigated as the second operating variable. Same as those observed for feed temperature, the increase the feed flow rate increased the permeation flux for both DCMD and SGMD modes. As it could be observed in Fig. 5, permeation flux was increased when the feed flow rate increased. It could be observed that elevating the feed flow rate was more effective for DCMD mode in comparison with SGMD mode. It can be explained by this fact that boundary

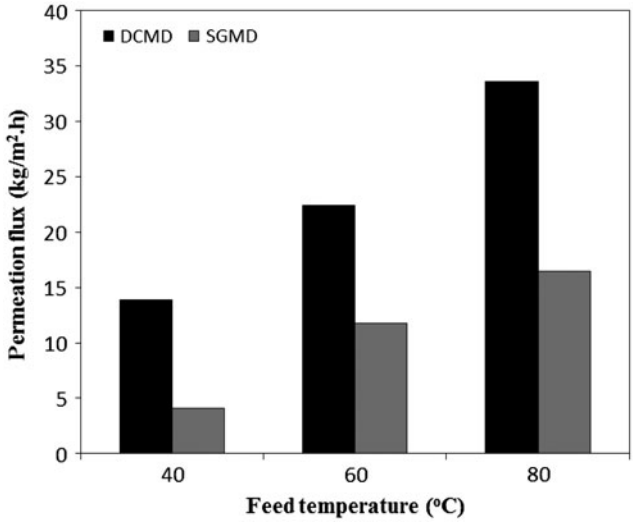

Fig. 4. Effect of feed temperature on the permeate flux through two configurations; DCMD (Q_h = 600 mL/min, T_c = 25 ± 2°C, and Q_c = 300 mL/min) and SGMD (Q_h = 600 mL/min, Q_a = 0.453 Nm^3/h); (C = 45 g/L).

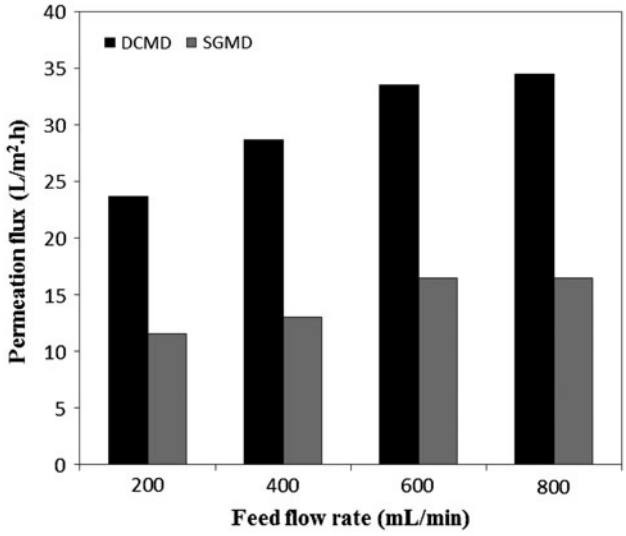

Fig. 5. Effect of feed flow rate on the permeate flux through two configurations; DCMD ($T_h = 80$ °C, $T_c = 25 \pm 2$ °C and $Q_c = 300$ mL/min) and SGMD ($T_h = 80$ °C, $Q_a = 0.453$ Nm^3/h); ($C = 45$ g/L).

layers effect reduced, especially for those of thermal boundary layers, which are of more influence in DCMD compared with the SGMD [8,9]. In other words, heat loss through thermal conduction of polymeric membrane is higher for DCMD, and this drawback may reduce with the use of higher feed flow rates. Moreover, feed temperature was more effective in comparison with the feed flow rate due to the nature of driving force in MD process (vapor pressure difference), which is in agreement to the previous works [17,20]. Based on the obtained results, a feed flow rate of 600 mL/min was adopted for next experiments.

A variety of the methods have been used to impose the driving force and improve the permeation flux in MD process; a flow of distilled water for DCMD and a flow of dried inert gas for SGMD, both in lower temperature and pressure compared to the feed-side conditions [26]. In order to evaluate the effect of operating conditions in the permeate side, cold stream flow rates of 100, 200, 300, and 400 mL/min for DCMD, and 0.113, 0.283, and 0.453 Nm^3/h for SGMD were considered, respectively. Fig. 6 shows the effect of cold stream flow rates in the permeate side of the MD module for DCMD and SGMD, respectively. Results indicated that increase in cold stream flow rate for DCMD led to increase in the permeation flux and this variation was almost linear. However, compared to the hot stream flow rate, the cold stream flow rate had less effect in DCMD (Fig. 6(a)). Based

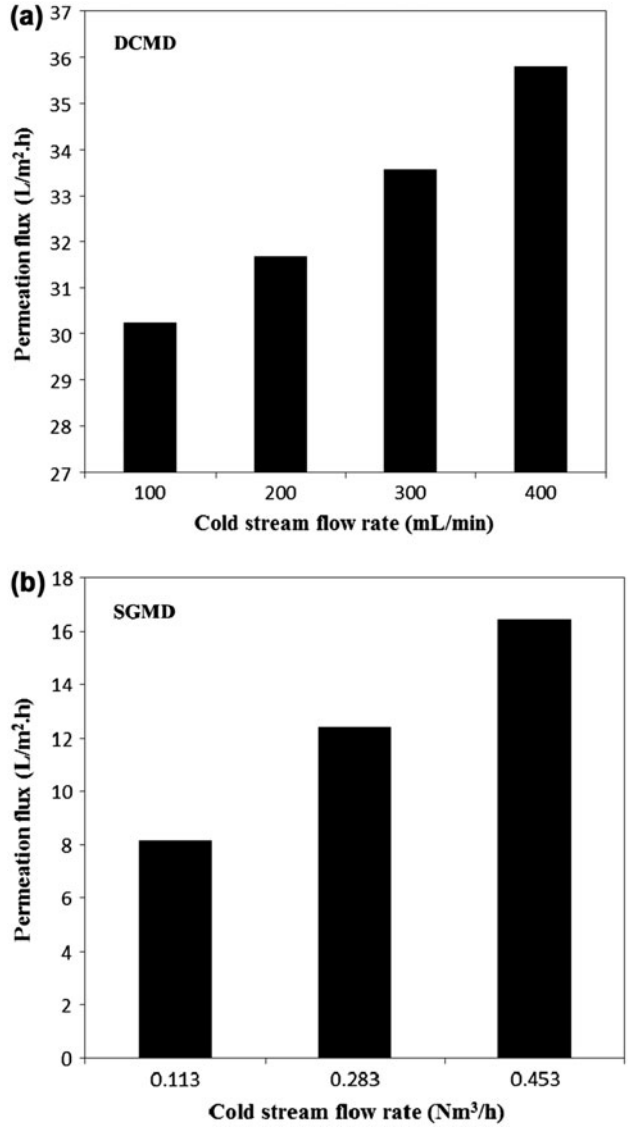

Fig. 6. Effect of cold stream flow rate on the permeation flux ($T_h = 80$ °C, $Q_h = 600$ mL/min, and $T_c = 25 \pm 2$ °C).

on the experimental results (Fig. 6(b)), the SG flow rate obviously affected the permeation flux; and the increase in the SG flow rate led to the increase in permeation flux. It is worth quoting that SG flow rate in the SGMD was more effective compared with the liquid cold stream flow rate in the DCMD. Moreover, the variation of the permeation flux was almost linear. These effects could be explained by this fact that same as those happened in the hose side, increase the cold stream flow rate caused to reduce the temperature polarization effect in the membrane surface. This may increase the temperature difference across the membrane, and consequently resulting higher driving force for the vapor transfer through the pores.

Although, it should be noted that providing higher flow rate, both in hot and cold side channels, required higher inlet pressure which may increase the risk of pore-wetting criteria. Based on the obtained results, cold stream flow rate (in DCMD) of 400 mL/min and SG flow rate (in SGMD) of 0.453 Nm^3/h were adopted for the next experiments.

Overall, it could be concluded that the permeation flux obtained by DCMD was significantly higher compared with the result obtained by SGMD as the same feed conditions. This point is so important, however, the reason has not yet been clearly addressed. Actually, as mentioned earlier, the main difference between the four major MD modes consists of the type of condensing design, a cold liquid stream in DCMD, and a cold gas stream in SGMD. It is obviously well-known that the capacity of the cold liquid stream for absorption and condensing the permeated vapor is significantly higher than that of cold air stream in SGMD. In other words, when the permeated vapor condenses in the membrane–cold air interface, the air stream is closed to be saturated by the hot vapor, whilst in the case of cold distilled water in DCMD, the condensing agent (cold liquid) is far from saturation state with the permeated vapor and its condensing capacity could be investigated infinity.

3.3. Effect of MD module design

Membrane module design, including hot and cold flows arrangement and feed and permeate channels' depth are important parameters determining the efficiency of the MD process which involves simultaneous heat and mass transfer phenomena [20,22]. Therefore, the arrangement of flows inside the MD module was investigated through three configurations, co-current, counter-current, and cross-current (Fig. 7), while the optimum operating conditions (80 °C and 600 mL/min for feed stream, 400 mL/min for DCMD, and 0.453 Nm^3/h for SGMD in permeate side, respectively), obtained from the previous section were considered. Results indicated that the higher permeation flux was observed by use of the cross-current flow arrangement for both DCMD and SGMD modes. These results could be observed in Fig. 8. Moreover, the counter-current flow arrangement led to higher permeation flux compared to the co-current flow. This could be explained as follows. As stated before, if the MD process is not an isothermal operation; then, the flow arrangement becomes important. In the co-current configuration, there is a maximum driving force at the module's entrance zone of the fluids, which is higher than the driving force for the counter-current configuration. However, this driving force decreases

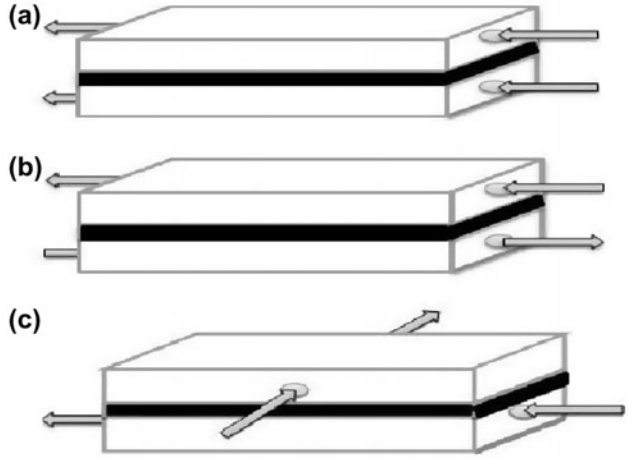

Fig. 7. The flow arrangement between hot and cold streams inside the MD module; (a) co-current, (b) counter-current, and (c) cross-current.

along the membrane, and it approaches zero if the fluid path is long enough. In contrast, the driving force for counter-current configuration is nearly constant, less than the force at module's entrance zone and higher than that at the exit zone of the co-current configuration. In counter-current arrangement, the system does not meet the equilibrium. The cross-flow configuration is more efficient than both co-current and counter-current ones. There is no doubt that the co-current arrangement is not as efficient as the

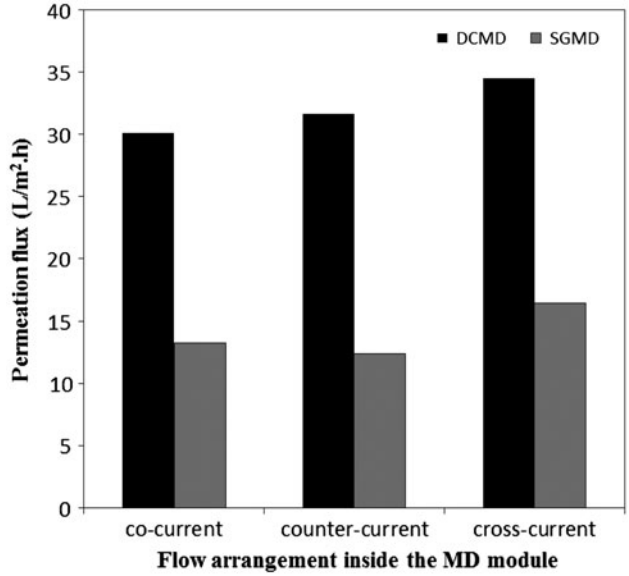

Fig. 8. Effect of flow arrangement on the permeation flux for DCMD ($T_h = 80$ °C, $Q_h = 600$ mL/min, $Q_a = 400$ mL/min, $T_c = 25 \pm 2$ °C), and SGMD ($T_h = 80$ °C, $Q_h = 600$ mL/min, $Q_a = 0.453$ Nm^3/h).

counter-current one due to lower overall driving force. This is one of the major reasons for the baffling of heat-exchangers that converts counter-current flow to more efficient cross-flow configuration. In the cross-flow arrangement, the system does not meet the equilibrium and the driving force is higher than both co- and counter-current configurations. This is because of the cascade nature of the cross-flow arrangement, where the hot stream always meets the fresh cold stream. In other words, this system is similar to infinite small cascade heat-exchangers in them and the driving force is at its maximum value. Consequently, the efficiency of both heat and mass transfer in such a cascade system could be more than in both co- and counter-current arrangements.

It is well-known that both temperature and concentration polarizations at the fluid–membrane interface are most important drawbacks of the MD process [9]. A practical strategy, in order to reduce the polarizations effect and improve the permeation flux is increasing the feed superficial velocity, which directly affects the thermal and concentration boundary layers in the feed–membrane interface [27]. The velocity may be varied by changing the flow channel depth while the flow rate remains constant. Fig. 9 indicates that increasing the flow channels' depth for both the feed and the permeate sides (from 2 to 6 mm) led to decrease of permeation flux, significantly. It is reasonable because increasng the flow channels' depth led to decrease in the superficial velocity, and consequently an increase in polarizations effect.

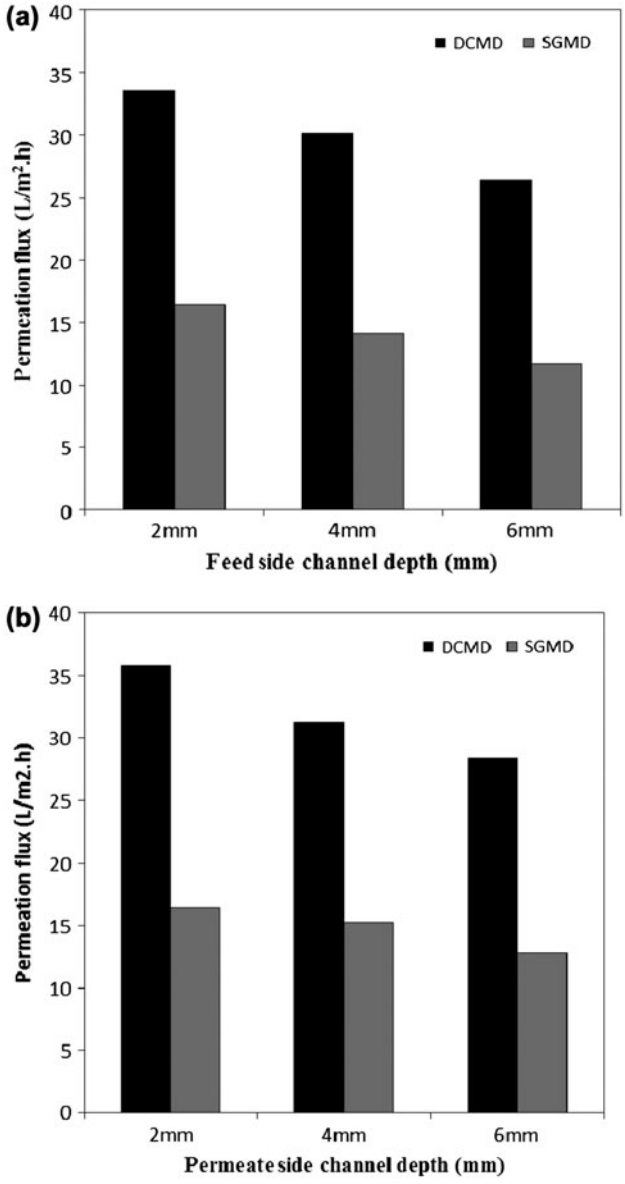

Fig. 9. Effect of feed channel depth (a) and permeate channel depth (b) on the permeation flux under the same operating conditions.

3.4. Effect of feed type

The performance of both MD modes was evaluated using synthesized and real Persian Gulf seawaters for 12 h and at the same operating conditions (the best operating conditions adopted from previous experiments). Samplings were performed every 30 min and a prefiltration step was applied for real seawater using PP capillary depth filter (5 μm pore size). The results are shown in Fig. 10 for both DCMD and SGMD. As could be observed for both modes, the permeation flux reduced as operating time increased. Moreover, this reduction in the permeation flux was more considerable for the real seawater sample when comparing with the synthesized feed sample. The main reasons for MD flux decline in long-term operations are scaling, pore-clogging, and biofouling [28,29]. Since the major constituents in seawater are alkaline (basic) deposit forming materials such as calcium or magnesium carbonates and diatomic earth; by lowering the pH of the feed water, these alkaline deposits become soluble and the scale formation is limited to acidic scalants such as siliceous compounds. But, other deposit-forming materials, such as silicates or sulfate compounds, and also solid particles can foul and clog the membrane and decline the flux. Biofouling is also important, especially when a natural origin feed such as seawater is used as the process liquid [29]. Extensive study on MD fouling reduction by reducing the feed stream's pH using HCl investigated in our previous work [18]. The results indicated that flux decline, either for treated or untreated seawater is completely reasonable, but it shows the need for monthly membrane cleaning.

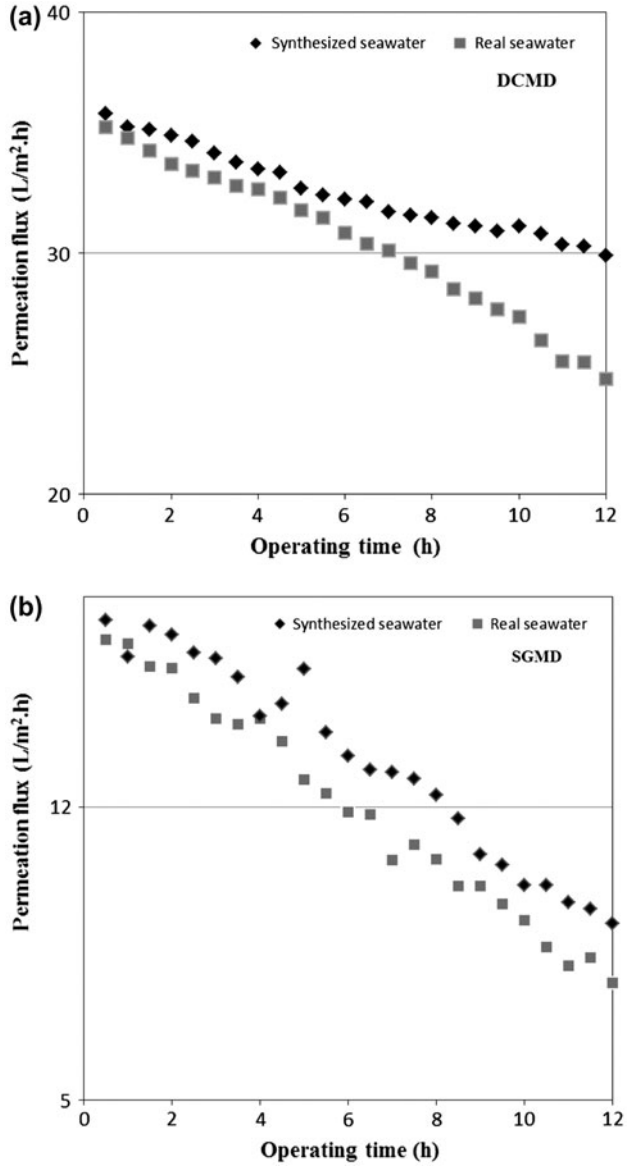

Fig. 10. Effect of feed type on the permeation flux during 12-h operation using (a) DCMD and (b) SGMD configurations.

The permeation flux variation for DCMD by use the synthesized seawater was almost linear and lower than that observed for the real seawater. Moreover, during the first 6 h, same variation of the permeation fluxes was observed for both feed samples. The initial and final permeation fluxes for synthesized and real seawater samples were 35.79 and 29.88 $L/m^2 h$; and 35.21 and 24.78 $L/m^2 h$, respectively. In contrast, DCMD which showed almost linear permeation flux variation, the flux obtained for SGMD was not linear for both feed waters, and more reduction was observed. The initial and final permeate flux for synthesized and real seawater samples in this case were 16.47 and 9.22 $L/m^2 h$; and 16 and 7.79 $L/m^2 h$, respectively.

4. Conclusions

In this work, two MD modes, the SGMD and the DCMD, were successfully investigated for the production of drinking water from synthesized and real Persian Gulf seawater. In both MD modes, the feed temperature had major effect on the permeation flux so that an increase of feed temperature increases the permeation flux exponentially. The DCMD shows better performance in comparison with SGMD. This was due to the higher condensing capacity in the permeating side of DCMD (which uses cooled water as the condensing agent) compared to the SGMD (which uses cooled air stream as the condensing agent). By proper selection of flow arrangement and superficial velocity of the streams, the polarization effects could be minimized. Among the three different flow arrangements, the cross-current mode offered the best performance for both the investigated modes. Scale formation is the major reason for flux decline during long-time runs. Periodical addition of acid and alkali to the feed solution may be considered as a practical method for online cleaning and flux recovery for this system. For both MD modes, 99.9% salt rejection was achieved.

Due to lower operating temperature, the ability to use the waste and/or renewable energy sources, i.e. solar, wind, etc., MD can be investigated for desalination purposes. Obviously, in the Persian Gulf region, due to high solar radiation, industrial MD plants have a promising future.

Acknowledgments

This work was partially supported by Young Researchers and Elites Club (Omidieh Branch) of Islamic Azad University which is acknowledged. Special thanks to Eng. Farhad Ghadyanlou, the head of R&D unit in Morvarid Petrochemical Co., for his useful help.

References

[1] F. Edwie, M.M. Teoh, T.S. Chung, Effects of additives on dual-layer hydrophobic-hydrophilic PVDF hollow fiber membranes for membrane distillation and continuous performance, Chem. Eng. Sci. 68 (2012) 567–578.
[2] P. Wang, M.M. Teoh, T.S. Chung, Morphological architecture of dual-layer hollow fiber for membrane distillation with higher desalination performance, Water Res. 45 (2011) 5489–5500.

[3] C. Feng, K.C. Khulbe, T. Matsuura, A.F. Ismail, Preparation and characterization of electro-spun nanofiber membranes and their possible applications in water treatment, Sep. Purif. Technol. 102 (2013) 118–135.
[4] L. Mar Camacho, L. Dumee, J. Zhang, J. Li, M. Duke, J. Gomez, S. Gray, Advances in membrane distillation for water desalination and purification applications, Water 5 (2013) 94–196.
[5] A.S. Hassan, H.E.S. Fath, Review and assessment of the newly developed MD for desalination processes, Desalin. Water Treat. 51 (2013) 574–585.
[6] K.W. Lawson, D.R. Lloyd, Membrane distillation, J. Membr. Sci. 124 (1999) 1–25.
[7] M.S. El-Bourawi, Z. Ding, R. Ma, M. Khayet, A framework for better understanding membrane distillation separation process, J. Membr. Sci. 285 (2006) 4–29.
[8] E. Curcio, E. Drioli, Membrane distillation and related operations—a review, Sep. Purif. Rev. 34 (2005) 35–86.
[9] M. Khayet, Membranes and theoretical modeling of membrane distillation: A review, Adv. Colloid Interface Sci. 164 (2011) 56–88.
[10] B. Jiao, A. Cassano, E. Drioli, Recent advantages on membrane processes for the concentration of fruit juices: A review, J. Food Eng. 63 (2004) 303–324.
[11] H. Susanto, Towards practical implementations of membrane distillation, Chem. Eng. Processing: Process Intensiv. 50 (2011) 139–150.
[12] A.M.K. El-Ghonemy, Water desalination systems powered by renewable energy sources: Review, Renewable Sustainable Energy Rev. 16 (2012) 1537–1556.
[13] A. Hepbasil, Z. Alsuhaibani, A key review on present status and future directions of solar energy studies and applications in Saudi Arabia, Renewable Sustainable Energy Rev. 15 (2012) 5021–5050.
[14] T. Mezher, H. Fath, Z. Abbas, A. Khaled, Techno-economic assessment and environmental impacts of desalination technologies, Desalination 266 (2011) 263–273.
[15] P. Alamdari, O. Nematollahi, M. Mirhosseini, Assessment of wind energy in Iran: A review, Renewable Sustainable Energy Rev. 16 (2012) 836–860.
[16] P. Alamdari, O. Nematollahi, A.A. Alemrajabi, Solar energy potentials in Iran: A review, Renewable Sustainable Energy Rev. 21 (2013) 778–788.
[17] D. Bastani, A. Kargari, M.M.A. Shirazi, Membrane distillation alternative for concentrating of glucose syrups, 20th International Congress of Chemical and Process Engineering (CHISA-2012), 25–29 August 2012, Prague, Czech Republic.
[18] M.M.A. Shirazi, A. Kargari, M.J.A. Shirazi, Direct contact membrane distillation for seawater desalination, Desalin. Water Treat. 49 (2012) 368–375.
[19] B.L. Pangarkar, P.V. Thorat, S.B. Parjane, R.M. Abhang, Performance evaluation of vaccum membrane distillation for desalination by using a flat sheet membrane, Desalin. Water Treat. 21 (2010) 328–334.
[20] K. He, H.J. Hwang, M.W. Woo, I.S. Moon, Air gap membrane distillation on the different types of membrane, Korean J. Chem. Eng. 28 (2011) 770–777.
[21] M.M.A. Shirazi, D. Bastani, A. Kargari, M. Tabatabaei, Characterization of polymeric membranes for membrane distillation using atomic force microscopy, Desalin. Water Treat. (2013), doi: 10.1080/19443994.2013.765365
[22] K. He, H.J. Hwang, M.W. Woo, I.S. Moon, Production of drinking water from saline water by direct contact membrane distillation (DCMD), J. Ind. Eng. Chem. 17 (2011) 41–48.
[23] L.D. Nghiem, F. Hildiner, F.I. Hai, T. Cath, Treatment of saline aqueous solutions using direct contact membrane distillation, Desalin. Water Treat. 32 (2011) 234–241.
[24] M. Khayet, J.I. Mengual, G. Zakrzewska-Trznadel, Direct contact membrane distillation for nuclear desalination. Part I: Review of membranes used in membrane distillation and methods for their characteristics, Int. J. Nucl. Desalin. 1 (2005) 435–449.
[25] M.J.A. Shirazi, S. Bazgir, M.M.A. Shirazi, S. Ramakrishna, Coalescing filtration of oily wastewaters: characterization and application of thermal treated, electrospun polystyrene filters, Desalin. Water Treat. (2013), doi: 10.1080/19443994.2013.765364
[26] P. Wang, T.-S. Chung, A conceptual demonstration of freeze desalination-membrane distillation (FD-MD) hybrid desalination process utilizing liquefied natural gas (LNG) cold energy, Water Res. 46 (2012) 4037–4052.
[27] A. Alkhudhiri, N. Darwish, N. Hilal, Produced water treatment: Application of air gap membrane distillation, Desalination 309 (2013) 46–51.
[28] E. Guillen-Burrieza, R. Thomas, B. Mansoor, D. Jhonson, N. Hilal, H. Arafat,Effect of dry-out on the fouling of the PVDF and PTFE membranes under conditions simulating intermittent seawater membrane distillation (SWMD), J. Membr. Sci. 438 (2013) 126–139.
[29] Sh. Goh, Q. Zhang, J. Zhang, D. McDougald, W.B. Krantz, Y. Liu, A.G. Fane, Impact of biofouling layer on the vapor pressure driving force and performance of a membrane distillation process, J. Membr. Sci. (2013), doi: 10.1016/j.memsci.2013.03.023